Journal of Mathematics Research
http: www.ccsenet.org/jmr
Vol. 1, No. 2
September 2009

Application of Coordinate Resistance Functions on Predicting of Critical Impact Energy of Projectile for Perforation Phenomenon on Concrete Structure

Ahmad Mujahid Ahmad Zaidi (Corresponding author)
Faculty of Mechanical and Manufacturing Engineering, Universiti Tun Hussein Onn Malaysia
86400 Parit Raja, Johore, Malaysia
E-mail: mujahid@uthm.edu.my

Ismail Abdul Rahman
Faculty of Civil and Environmental Engineering
Faculty of Mechanical and Manufacturing Engineering, Universiti Tun Hussein Onn Malaysia
86400 Parit Raja, Johore, Malaysia
E-mail: ismailar@uthm.edu.my

Qadir Bux Alias Imran Latif
Faculty of Civil and Environmental Engineering
Faculty of Mechanical and Manufacturing Engineering, Universiti Tun Hussein Onn Malaysia
86400 Parit Raja, Johore, Malaysia

Mohd Imran Ghazali
Faculty of Mechanical and Manufacturing Engineering
Universiti Tun Hussein Onn Malaysia 86400 Parit Raja, Johore, Malaysia
E-mail: mujahid@uthm.edu.my

Abstract

Great demand exist for more efficient design to protect personals and critical components against impact by kinetic missiles, generated both accidentally and deliberately, in various impact and blast scenarios in both civilian and military activities. In many cases, projectiles can be treated as rigid bodies when their damage and erosion are not severe. Due to the intricacy of the local impact damages, investigations are generally based on experimental data. Conclusions of the experimental observations are then used to guide engineering models. Local damages studies normally fall into three categories, i.e. empirical formulae based on data fitting, idealised analytical models based on physic laws and numerical simulations based on computational mechanics and material models. Perforation phenomenon is one of the local damage that has been investigated in the present study. It is describe as the complete passage of the projectile through the material with or without residual velocity is among the local damage threat in concrete structure. The relative of target thickness (H/d) to those critical energies are an important quantities that been explored in this study. The numerical simulation model has been developed using coordinate resistance function method for predict the perforation process. The target structures is described based on coordinate system in a mesh-less way, which impose penetration resistance on the projectile through resistance function based on dynamic cavity expansion theory. The penetration resistance on the surface of the rigid projectile is a function of the instantaneous velocity of that surface, which can be determined by the rigid body motion of the projectile. Standard finite element method is introduced to model the rigid body motion of the projectile and is coupled with the coordinate resistance in a mesh-less target by exchanging the velocities and stresses through user-

interfaces. Predictions of the critical impact energies during perforation process are compared with semi-empirical model and corresponding experimental data. Encouraging predictions are observed when the model was validated with the existing experimental data.

Keywords: Critical impact energies, Perforation, Rigid projectile, Target thickness, Coordinate system

1. Introduction

Perforation phenomenon in concrete medium is described as a complete passage of the projectile through the concrete target with or without the residual velocity. It may occur when the kinetic energy of the projectile is sufficient to perforate the target medium. Due to its great demands especially in designing the protective components against kinetics missile which may generated both accidentally or deliberately, in various impact scenarios, the investigation of perforation phenomenon has attracted more interest in both civilian and military activities for the last century.

The latest state-of-the-art reviews can be found in Li et. al (2005) which summarised the recent progresses about the local impact including perforation and cover the major issues in empirical, analytical and numerical simulation. However due to the complexity of the studies, investigations are largely based on experimental data, which were then formulated to guide the design and assessment of concrete structures against impact and blast loads. Experimental investigation is a practical tool to studies the perforation mechanisms, which these mechanisms are forced by material behaviour and failure modes of the target structure. General behaviour of perforation mechanisms for brittle and ductile targets with various range of thickness can be found in Backman and Goldsmith (1978). They had illustrated eight possible perforation mechanisms as shown in Figure 1. Sugano et al. (1993) have demonstrated failure modes of concrete target in perforation phenomenon (as shown in Figure 2). From these experimental evidences, it is understood that the perforation phenomenon is mainly affected by two factors, i.e., the local effect and the structural response. The local effect is the local reactions of the target to the projectile impact without the influence of structural response of the target. Whilst the structural response is the reaction through the thickness of the target, which are caused by bending, transverse shear and membrane deformations, due to the complex wave reflections at its boundaries condition. Besides that, the experimental results can be further used to determine the perforation limit by empirically based on its fitted data and the latest review of these empirical formulae can be found in Li et al. (2005). However, these empirical formulae are limited based on their range of application.

< Figure 1 >

< Figure 2 >

Application of numerical simulations in perforation phenomenon has become increasingly important for the structure design. This is due to the computer capability and computational mechanics are significantly progressed. Several of the numerical simulations results demonstrated good predictions of some phenomena occurred during perforation process, e.g. penetration process(Warren(2002), Warren et al. (2004)) residual velocity and structural behaviours(Tham (2005), Huang et al. (2005), Polanco-Loria et al. (2008) and Teng et al. (2008)). Nevertheless, the fragmentation of the material target is still difficult to be numerically reproduced, which further investigation is needed.

Most of the analytical approaches in perforation phenomenon, generally assume that the projectile is rigid and the target is response based on its modes of deformation at several stages, i.e. penetration and shear plugging (Yankelevsky (1997), Li and Tong (2003)). For the penetration stage, the most of the models applied dynamic cavity expansion to measure the stress field and the penetration resistance. Forrestal et al. (1994), Forrestal et al. (1996), Frew et al. (1998) and Li and Chen (2003) employed the dynamic cavity expansion theory in penetration analysis of concrete target and demonstrated good agreement with experimental data. The shear plugging stage is involving two type of mechanisms, which are plug formation and shear during plugging (e.g. in Yankelevsky (1997) and Li and Tong (2003)). According to Li and Tong (2003), the transition between penetration and shear plugging stage occurs when the total penetration resistance force is equal to the shear resistance force provided by the remaining thickness of the target. However, it is note that the success of these analytical models is limited by its valid application ranges, partially due to the fact that most analytical models rely heavily on observations and assumptions over a narrow range of experimental parameters.

In this paper, the influences of the relative target thickness (H/d) on critical impact energy of perforation in various forms of concrete targets were explored. A dimensional analysis has been conducted for further application in predictions analysis. The numerical simulation, which is based on rigid dynamic motion, has been conducted with several of the target thickness. Predictions of the critical impact energies of perforation are compared with semi-empirical model and corresponding experimental data from Bainbridge (1988).

2. Dimensional Analysis

It is useful and important to consider the mechanics of the impact processes and thus deduce the relevant non-dimensional numbers that could be involved in perforation analyses. When a non-deformable, flat-nosed projectile strikes a concrete target, penetration process could occur due to the efficient kinetic energy. Then if the damage is sufficient, the process will lead to either completes perforation or the overall structural response. Therefore, the perforation limit, i.e. the minimum target thickness to prevent perforation, is generally defined by

$$e = fn(M,\ V_0,\ d,\ \rho,\ f_c,\ f_t,\ ,\tau_f,\ E,\ a,\ r) \tag{1}$$

where *rho*, E, τ_f, f_c and f_t are the density, Young's modulus, shear strength, unconfined compressive and tensile strengths (stresses) of the concrete target, respectively. a is the characteristic size of aggregate and r is the average percentage amount of reinforcement each-way-each-face (ewef). M and V_0 are the mass and the initial impact velocity of a projectile and d is the (cylindrical) projectile shank diameter.

Most of the published empirical formulae for local damage phenomena (i.e., penetration, perforation and scabbing) does not explicitly account for the amount of reinforcement and aggregate. It has been shown that light or moderate reinforcement (i.e. $r = 0.3\% - 1.5\%$ ewef has little effect on penetration and scabbing). Thus, when the aggregate size and the amount of reinforcement are neglected, a dimensional analysis based on Equation (1) leads to

$$\frac{e}{d} = fn\Big(\frac{E_k}{d^3 f_c},\ \frac{M}{\rho d^3},\ \frac{f_t}{f_c},\ \frac{\tau_f}{f_c},\ \frac{E}{f_c}\Big) \tag{2}$$

where $E_k = \frac{1}{2}MV_0^2$ is the kinetic energy of the projectile.

Although the perforation limit is normally selected as a design parameter in empirical formulae, the critical impact velocity to cause perforation for given target thickness is another important parameter associated with perforation. The critical impact energy can be expressed by

$$\frac{E_c}{d^3 f_c} = fn\Big(\frac{M}{\rho d^3},\ \frac{H}{d},\ \frac{f_t}{f_c},\ \frac{E}{f_c},\ \frac{\tau_f}{f_c} \tag{3}$$

where H is the thickness of the concrete target and $E_c = \frac{1}{2}MV_c^2$. For a given target, $\frac{f_t}{f_c}$, $\frac{\tau_f}{f-c}$ and $\frac{E}{f_c}$ may be considered as constants.

In subsequent presentations of experimental data and numerical simulation predictions, the above non-dimensional groups will be employed. Analytical models will offer further support and provide more explicit expression of these results.

3. Numerical Simulation Model

The complete perforation process is modeled using the ABAQUS finite element software package. It is note that only the penetration mechanism is considered in the simulation model, where the perforation occurs when the penetration depth is equal to the target thickness. Another possible mechanism of shear plugging is not significant for the thick target. For the simplification, the two-dimensional axisymmetric approach is adapted in the numerical model of perforation. The projectile is modeled in standard finite element with flat nose shape and has been treated as a discrete rigid body with element type RAX2 (2-node, reduce-integration and axisymmetric). The concrete target is modeled as a mesh-less layer (based on coordinate resistance function), which imposes pressure resistance on the projectile surface through resistance function. The resistance on the surface of rigid projectile is a function of the instantaneous velocity of projectile nose surface, which can be determined by the rigid motion of the projectile. Coupling between the motion of rigid projectile and the mesh-less target is made by exchanging the velocities and stresses through a user-interface in ABAQUS using Compaq Visual FORTRAN 6 software. More details are described below.

3.1 Assumption and boundary condition

The projectile is assumed to be a rigid body, i.e., its deformation is negligible during perforation process. The projectile is assumed to strike the target at the normal incident angle and the friction between the projectile surface and the concrete target is neglected as a secondary effect.

The concrete target is described in a mesh-less way (based on coordinate resistance function). Both projectile and target medium are defined under a common coordinate system. The resistance function is applied when the projectile has entered the target domain and it will stop when the projectile passed through the target medium (which this is pre-defined in the coordinate system), as shown in Figure 3. The resistance function for the concrete is derived from the cavity expansion theory, which is given by (Li and Chen(2003)), i.e.,

$$F = cx \quad for\ x < kd \tag{4}$$

$$F = \frac{\pi d^2}{4}(\tau_0 A + N * B\rho_c V^2) \quad for\ x \geq kd \tag{5}$$

where c is a constant, τ_0 is the shear strength of concrete target, A and B are concrete material constant and V is the instantaneous velocity of the projectile. It is noted that in this model, the interface friction between the projectile nose and concrete medium is neglected.

The Equation (4)-(5) is used to define the normal resistant pressure imposed on projectile surface by the foamed concrete target (e.g. in Figure 3, the resistance pressure from Equations (4)-(5) will be applied based on to their boundary condition).

< Figure 3 >

3.2 Explicit dynamic finite element algorithm in simulation model

The explicit dynamics analysis procedure is based upon the implementation of an explicit integration rule together with the use of diagonal or "lumped" element mass matrices. The equations of motion for the body (projectile) are integrated using the explicit central difference integration rule.

$$V^{(i+1/2)} = V^{(i-1/2)} + [(\triangle t^{(i+1)} + \triangle t^{(i)})/2]a^{(i)} \tag{6}$$

$$U^{(i+1)} = U^{(i)} + \triangle t^{i+1} V^{(i+1/2)} \tag{7}$$

where U is displacement, V is velocity and a is acceleration. The superscript (i) refers to the increment number and $(i - 1/2)$ and $(i + 1/2)$ refer to midincrement values. The central difference integration operator is explicit in that the kinematic state can be advanced using known values of $V^{(i-1/2)}$ and $a^{(i)}$ from previous increment. The computational efficiency of the explicit procedure is depend on using the diagonal element mass matrices because of the inversion of the mass matrix that is used in the computation for the accelerations at the beginning of the increment is triaxial;

$$a^{(i)} = M^{-1} \triangle F \tag{8}$$

where are;

$$\triangle F = (F)^{(i)} - I^{(i)} \tag{9}$$

$$(F^{(i)}) - I^{(i)} = \sigma^{(i)} S \tag{10}$$

M is the diagonal lumped mass matrix, S is the front nose's projectile surface, F is the applied force vector, I is the internal force vector and $\sigma^{(i)}$ is determined by Eq. (4) and (5).

4. Semi-Empirical Model

This predictive semi-empirical model was developed by Li et. al (2006). The values for the non-dimensional penetration depth x/d for $V_0 << \sqrt{\frac{S f_c}{\rho}}$ and $\frac{M}{\rho d^3} >> 1$ are given by

$$\frac{X}{d} = \sqrt{\frac{4k}{\pi} I},\ for\ \frac{X}{d} \leq k\ or\ I \leq \frac{k\pi}{4} \tag{11}$$

and

$$\frac{X}{d} = \frac{k}{2} + \frac{2I}{\pi},\ for\ \frac{X}{d} > k\ or\ I > \frac{k\pi}{4} \tag{12}$$

where k=2 will be used in subsequent evaluations and calculations as suggested by Li and Tong (2003). The impact function I and geometry function are given by

$$I = \frac{1}{S}\left(\frac{MV_0^2}{d^3 f_c}\right) = \frac{2}{S}\left(\frac{E_k}{d^3 f_c}\right)\ and\ N = \frac{M}{\rho d^3} \tag{13}$$

where S is a non-dimensional number (the units for fc are MPa) given by

$$S = 72.0 f_c^{-0.5} \tag{14}$$

Equations (11-12) correspond to $N >> I$ and $N >> 1$ where I and N are given in Eqs.(13), which are normally satisfied in the experiments of interest.

The critical impact energy for perforation, denoted by E_{cp}, can be derived from the above equations when the perforation limit equal the target thickness H and the non-dimensional numbers in Equation (3) is employed, i.e.,

$$\begin{aligned}
\frac{E_{cp}}{d^3 f_c} &= 0.196S\,[2.222 - \sqrt{4.935 - 1.393\frac{H}{d}}]^2 && for\ \frac{H}{d} \leq 3.0 \\
\frac{E_{cp}}{d^3 f_c} &= 0.128S\left(\frac{H}{d} - 1.320\right)^2 && for\ 3.0 < \frac{H}{d} \leq 3.80 \\
\frac{E_{cp}}{d^3 f_c} &= 0.633S\left(\frac{H}{d} - 2.560\right) && for\ 3.80 < \frac{H}{d} < 18.0
\end{aligned} \tag{15}$$

5. Results and Discussion

For validation purposes, semi empirical formula results and numerical simulation results are compared with experimental data obtained by Bainbridge (1988), as shown in Figure 4.

<Figure 4>

From the Figure 4, it is shown that semi-empirical predictions give better agreement with the experimental data than simulation predictions. The simulation results over-predict the critical impact energy because perforation normally occurs before the penetration depth reaches the target thickness. It is noted that at a thin to medium target, the shear plugging effect contributes significantly in perforation process, which is shown at $\frac{H}{d} \leq 3.0$, where simulation predictions are greater than corresponding experimental data. However, with increase of target thickness especially when $\frac{H}{d} \geq 3.0$, the difference between simulation and experimental results is reduced gradually, as shown by the percentage difference between experimental data and simulation results, as shown in Figure 5. This indicates that shear plugging mechanism is less significant for the thick target.

<Figure 5>

Figure 5. Percentage different between simulation and experimental data

In general all predicted results are following the general trend of experimental data, which are shows that the semi-empirical predictions provide the lower bound of experimental data and the simulation predictions provide the upper bound of experimental data. However, due to the scatter in the experimental data, the applications of the semi empirical model as well as simulation predictions should be combined with a properly selected safety factor.

6. Conclusions

The influence of the relative target thickness (H/d) on the critical impact energies for perforation in concrete targets has been investigated. A dimensional analysis was conducted to identify influential non-dimensional numbers, which were subsequently employed in further results analysis. Simulation model based on rigid body motion with consideration of penetration effects as a perforation criterion has been developed to further provide critical impact energies prediction along with selected semi-empirical model. Predictions based on these predictive models have been compared with the experimental data in Bainbridge(1988) and generally those predictions results gives good correlation with experimental results. Among those predictions, simulation model has over-predicted experimental data and semi-empirical results provide the lower bound of experimental data. It is concluded that an appropriate safety factor should be considered for applying those predictive models.

References

Backmann, M.E. and Goldsmith, W. (1978). The mechanics of penetration of projectiles into targets. *Int. J. Eng. Sci.*, 16, pp. 1-99.

Forrestal, M.J., Altman, B.S., Cargile, J.D. and Hanchak, S.J. (1994). An empirical equation for penetration depth of ogive-nose projectilesinto concrete targets. *Int. J. Impact Eng.*,15(4), pp. 395-405.

Forrestal, M.J., Frew, D.J., Hanchak, S.J. and Brar, N.S. (1996). Penetration of grout and concrete targets with ogive-nose steel projectiles. *Int. J. Impact Eng.*, 18(5):465-76.

Frew, D.J., Hanchak, S.J., Green, M.L. and Forrestal, M.J. (1998). Penetration of concrete targets with ogive-nose steel rods. *Int. J. Impact Eng.*, 21, pp. 489-497.

Huang, F., Wu, H., Jin, Q. and Zhang, Q. (2005). A numerical simulation on the perforation of reinforced concrete targets. *Int. J. Impact Eng.*, 32, pp. 173-187.

Isao Kojima. (1991). An experimental study on local behaviour of reinforced concrete slabs to missile impact. *J. Nuc. Eng. Des.*, 130(2), pp. 121-132.

Li, Q.M. and Chen, X.W. (2003). Dimensionless formulae for penetration depth of concrete target impacted by a nondeformable projectile. *Int. J. Impact Eng.*, 28(1), pp. 93-116.

Li, Q.M. and Tong, D.J. (2003), Perforation thickness and ballistic performance of concrete target subjected to rigid projectile impact. *ASCE J. Eng. Mech.*, 129(9), pp. 1083-91.

Li, Q.M., Reid, S.R., Wen, H.M. and Telford, A.R. (2005). Local impact effects of hard missiles on concrete targets. *Int. J. Impact Eng.*, 32, pp. 224-284.

Polanco-Loria, M., Hopperstad, O.S., Borvik, T. and Berstad, T. (2008). Numerical predictions of ballistic limits for concrete slabs using a modified version of the HJC concrete model. *Int. J. Impact Eng.* (in press).

Sugano, T., Tsubota, H., Kasai, Y., Koshika, N., Ohnuma, H., Von Riesemann, W.A., Bickel, D.C. and Parks, M.B. (1993). Local damage to reinforced concrete structures caused by impact of aircraft engine missiles Part1: Test program, method

and results. *J. Nuc. Eng. Des.*, 140, pp. 387-405.

Teng, T.L., Chu, Y.A., Chang, F.A., Shen, B.C. and Cheng, D.S. (2008). Development and validation of numerical model of steel fiber reinforced concrete for high-velocity impact. *Computational Materials Science* (in press).

Tham, C.Y. (2005). Reinforced concrete perforation and penetration simulation using AUTODYN-3D. *Finite Elements in Analysis and Design*, 41, pp. 1401-1410.

Warren, T.L. (2002). Simulations of the penetration of limestone targets by ogive-nose 4340 steel projectiles. *Int. J. Impact Eng.*, 27, pp. 475-496.

Warren, T.L., Fossum, A.F. and Frew, D.J. (2004). Penetration into low-strength (23MPa) concrete: target characterization and simulations. *Int. J. Impact Eng.*, 30, pp. 477-503.

Yankelevsky, D.Z. (1997). Local response of concrete slabs to low velocity missile impact. *Int. J. Impact Eng.*, 19(4), pp. 331-343.

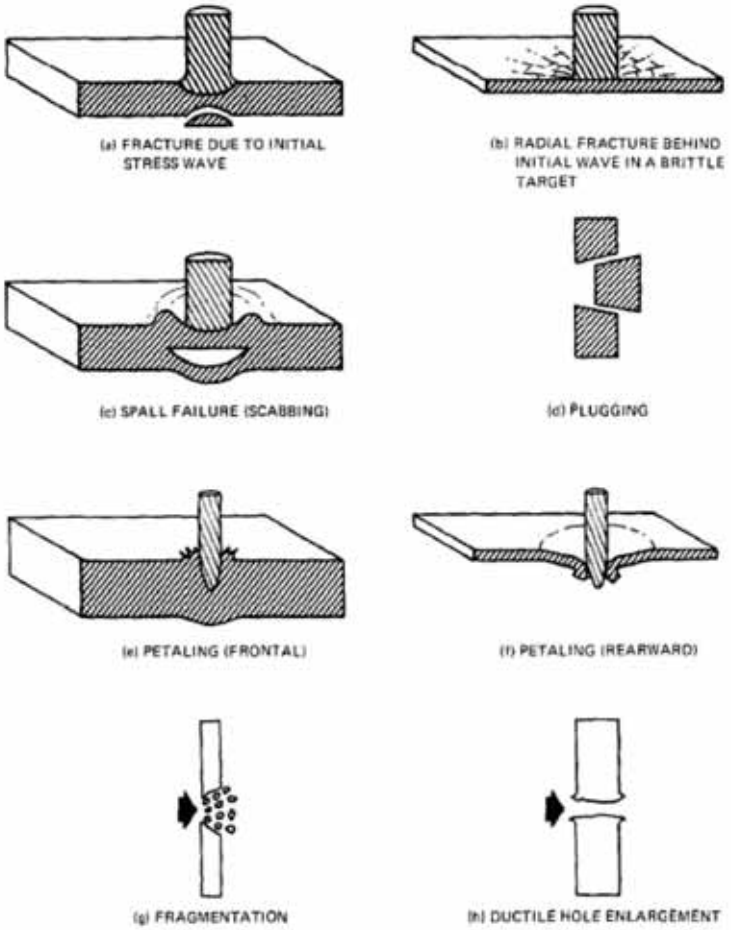

Figure 1. Perforation mechanisms in ductile and brittle materials [Backman and Goldsmith(1978)]

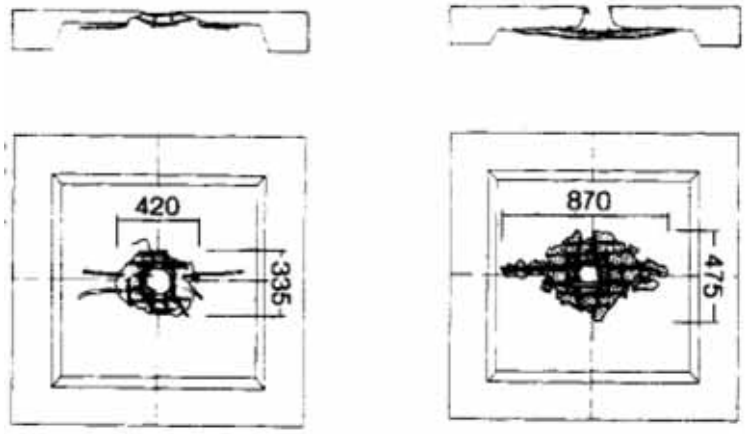

Figure 2. Experimental illustration of (a) perforation, (b) just perforation [Sugano et al.(1993)]

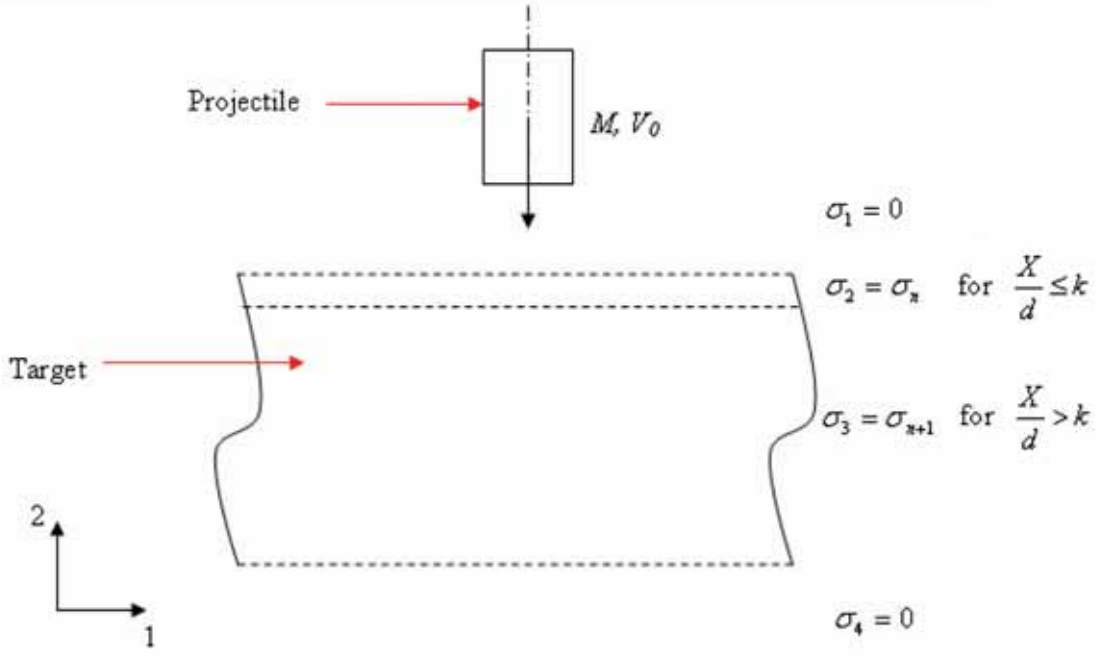

Figure 3. Boundary condition of perforation model

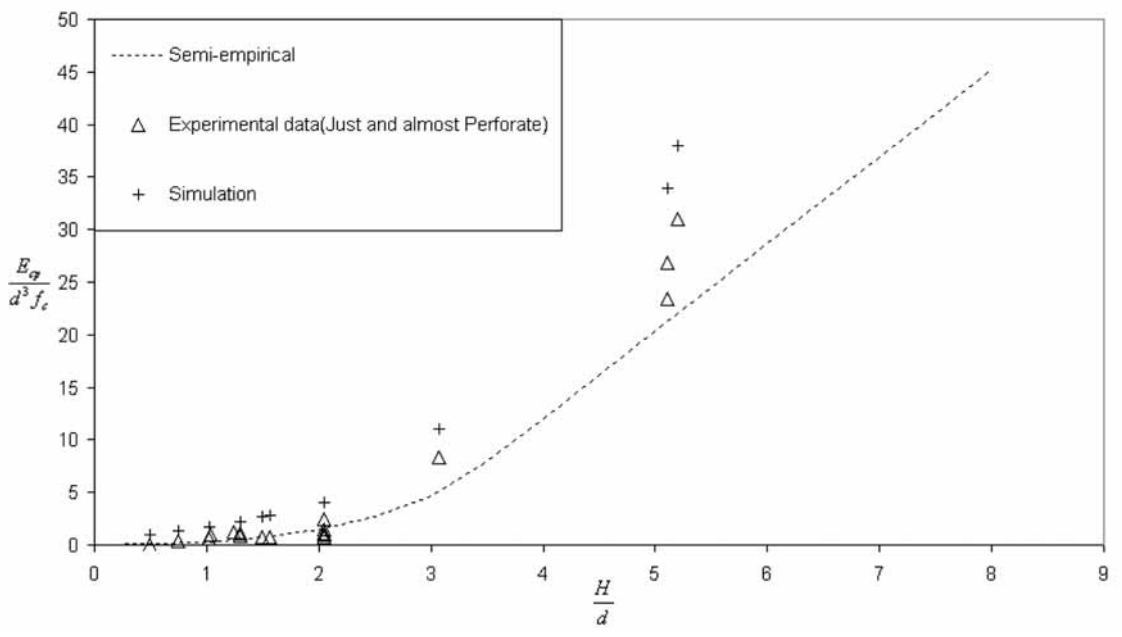

Figure 4. Comparisons between semi-empirical formula, simulation predictions and experimental data (just and almost perforated tests) for perforation [experimental data: Bainbridge(1988), semi-empirical: Equation(15a-c)]

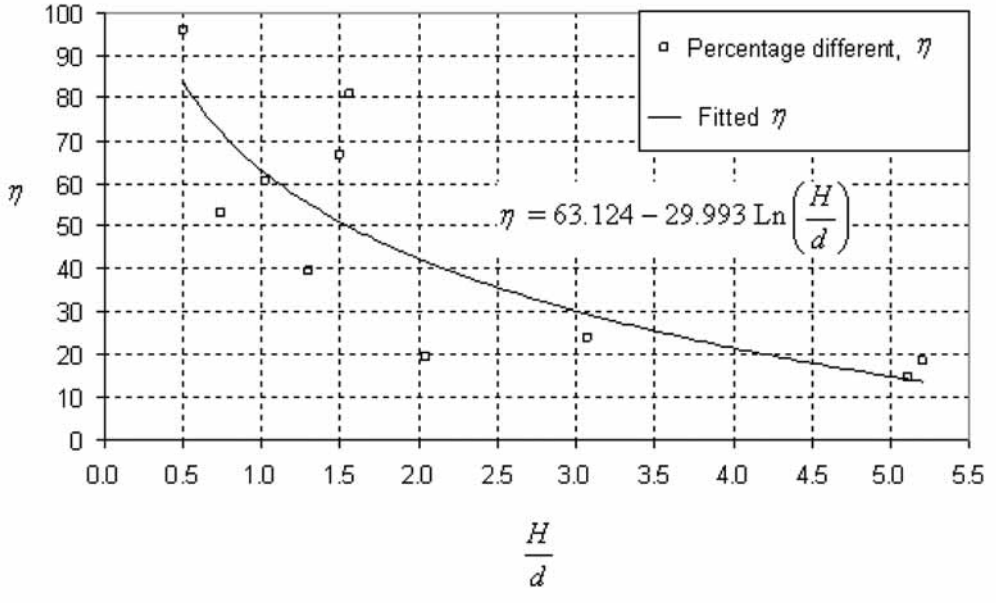

Figure 5. Percentage different between simulation and experimental data